# DEM Extraction from High Resolution Imagery♥

Thierry Toutin
Canada Centre for Remote Sensing, Natural Resources Canada
588, Booth Street, Ottawa, Ontario K1A 0Y7 Canada
Thierry.toutin@ccrs.nrcan.gc.ca

***Abstract-*** Digital elevation models (DEMs) extracted from high-resolution stereo images (SPOT-5, EROS and IKONOS) using a three-dimensional (3-D) multi-sensor physical model developed at the Canada Centre for Remote Sensing, Natural Resources Canada were evaluated. Firstly, the photogrammetric stereo-bundle adjustment was set-up with few accurate ground control points. DEMs were then generated using an area-based multi-scale image matching method and then compared to 0.2-m accurate lidar elevation data. Elevation linear errors with 68% confidence level (LE68) of 6.5 m, 20 m and 6.4 m were achieved for SPOT, EROS and IKONOS, respectively. The worse results for EROS are mainly due to its asynchronous orbit, which generate large geometric and radiometric differences between the stereo-images. When these differences are not large (such as in the middle of the stereo-pair), 10-m LE68 was achieved. Since SPOT and IKONOS DEMs were in fact a digital terrain surface model where the elevation of land covers (trees, houses) is included, the elevation accuracy is performed depending on the land cover types. LE68 of 1-2 m were obtained for bare surfaces and lakes. However, when compared to sensor resolution, SPOT achieved better results than IKONOS: half-pixel versus 1.5 pixels. On the other hand, LE68 of 4 m to 6.6 m were obtained depending on the forest types (deciduous, conifer, mixed or sparse) and its surface elevation.

## 1 INTRODUCTION

Since 1999, push-broom high-resolution (HR) satellite scanners have been launched with sensor resolutions in panchromatic mode ranging from 0.61 m (QuickBird) to 5 m (SPOT-5). Most of them (EROS-A, IKONOS, QuickBird and Orbview) are agile satellites (off-nadir viewing capability up to 60º in any azimuth), which enable same-date in-track stereo viewing, while SPOT-5 with its HRG sensors kept its traditional multi-date across-track stereo viewing. Same-date in-track stereo-data acquisition gives a strong advantage to multi-date across-track stereo-data acquisition because it reduces radiometric image variations (temporal changes, sun illumination, etc.), and thus increases the correlation success rate in any image matching process (Toutin, 2000). Both acquisition methods can generate strong stereo geometry with base-to-height ratio (*B/H*) of one, and users can then apply three-dimensional (3-D) photogrammetric methods with the stereo-images to extract accurate planimetric and elevation information, such as digital elevation models (DEMs).

♥ *Published in Geospatial Today, Vol. 2, Issue 3, July-August 2003.*
*Short version of a paper submitted to IEEE-IGARS.*

## 2 DESCRIPTION OF THE METHOD

### 2.1 Study Site and HR Stereo Data

The study site is an area north of Québec City, Québec, Canada (N 47º, W 71º 30'). The St Lawrence River is on the southwest part (Fig. 1). This study site is an urban/residential environment in the southern part with 85% covered by forests (deciduous, conifer and mixed) and has a hilly topography (1000-m elevation range and 10º mean slope). Only three HR stereo images were fully processed over this study site with *B/H* ratio of around one: raw level-1A SPOT-5 (5 m) and EROS-A (1.8 m) and Geo-product IKONOS (0.8 m) (Table I). The SPOT-5 (2.5 m) and QuickBird (0.61 m) stereo-pairs are being processed. Unfortunately, the images were generally acquired during the Canadian wintertime (January to May) with snow and ice and also with low sun illumination angles, 19° and 26° for EROS and IKONOS respectively, resulting in long shadows (Fig. 2 and 3). Even the SPOT data acquired May 5 (Fig. 1) displays more than 50% of melting snow in the forests (upper-left), frozen lakes or with significant melting ice (lower left and center), generating thus large radiometric differences in the stereo-pair. This gives, however, an opportunity to test the method and address the potential problems in a quasi-operational environment as well as to evaluate the results in such difficult conditions instead of working in a perfect well-controlled environment. SPOT-5 and IKONOS are synchronous satellites (Bouillon *et al.*, 2002; Dial, 2000) while EROS satellites are asynchronous (Chen and Teo, 2002). Since EROS is thus "too fast", it must continuously pitch backward during the image acquisition and the ground resolution is changing continuously (from 1.8 to 2.2 m).

Table I: Characteristics of the stereo pairs acquired over the Quebec study site, Canada.

| Stereo pair | Acquisition Date | Sun angle | Stereo | Viewing angles | Image (km) | Pixel (m) | Nb. GCPs |
|---|---|---|---|---|---|---|---|
| **SPOT-5 HRG** | May 05 2003<br>May 25 2003 | 52º<br>55º | Multidate Across | + 23º<br>-19º | 60 x 60 | 5 x 5 | 33 |
| **EROS-A Pan** | February 6 2002 | 24º | Same date Along | + 30º to +8º<br>- 6º to -27º | 13 x 13 | 1.8 to 2.4 | 130 |
| **IKONOS Pan** | January 3 2001 | 19º | Same date Along | ±27º | 10 x 10 | 1 x 1 | 55 |

Ground control points (GCPs) were collected in stereoscopy for the different tests on the bundle adjustment of the stereoscopic pairs. For SPOT-5 and EROS-A, GCP cartographic coordinates (*X*, Y, *Z*) were obtained from 1:20,000 digital topographic maps of the *Ministère des Ressources naturelles du Québec*, Canada. The accuracy is estimated to be around 2 m in planimetry and 3 m in elevation. Due to the better resolution of IKONOS sensor, GCP cartographic coordinates (*X*, Y, *Z*) were stereo-compiled using a Wild A-10 by the same *Ministère* from aero-triangulated 1:40,000 photos. The accuracy is estimated to be better than 1-m and 2-m in planimetry and elevation, respectively. To perform accuracy evaluation of the stereo-extracted DEMs,

accurate spot elevation data was obtained September 6th, 2001 from a lidar survey by GPR Consultants (www.lasermap.com) using an Optech ALTM-1020 system. Since it was impossible to cover the full SPOT coverage (60 km by 60 km), ten swaths were only acquired covering an area of 5 km by 13 km, which is representative of the full study site. The results are then an irregular-spacing grid (around 3 m), due also to no echo return in some conditions (buildings with black roof, some roads and lakes).

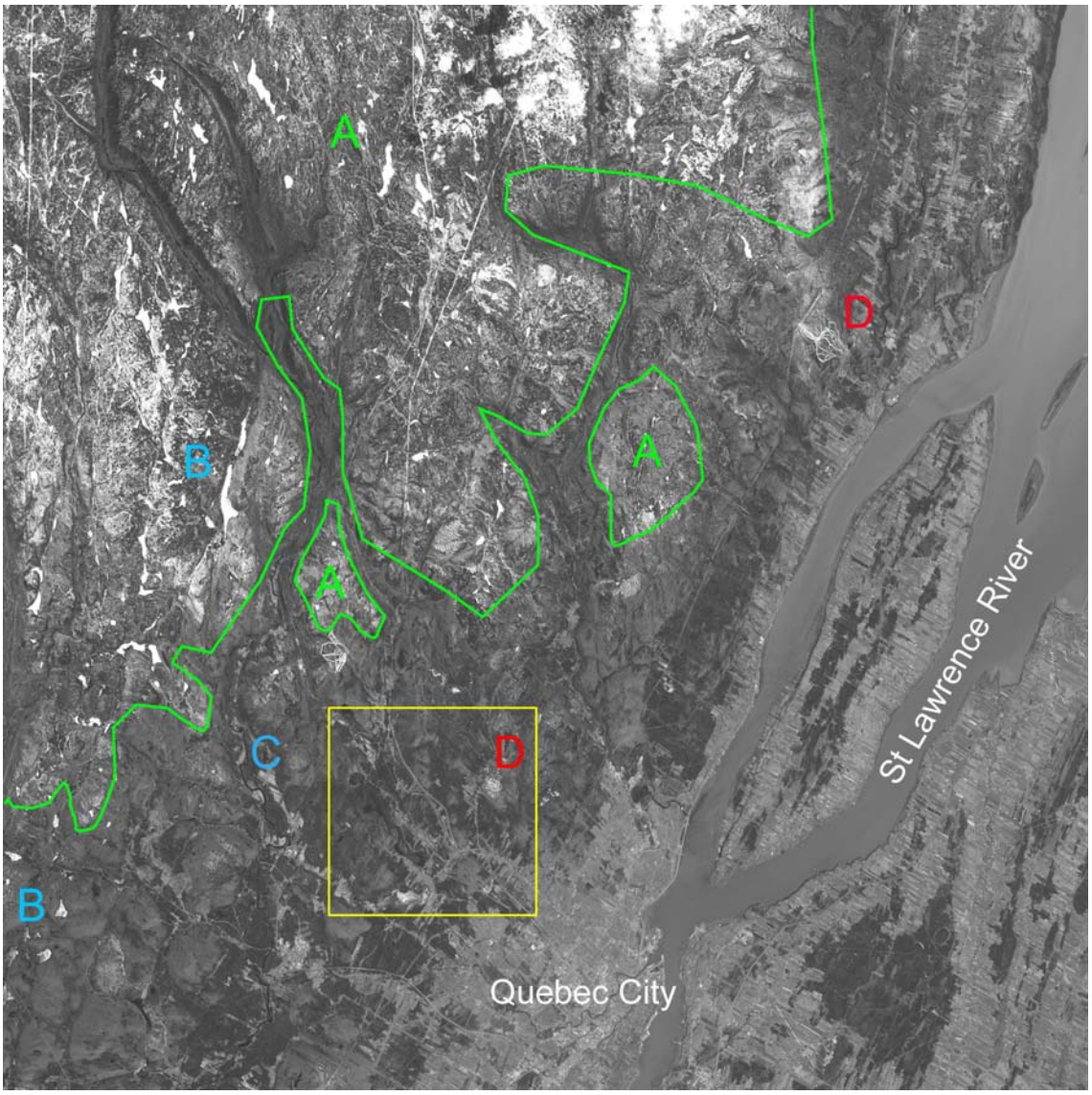


**Figure 1.** SPOT-5 HRG image (May 5 2003; 23° west-viewing angle; 60 km by 60 km; 5-m pixel spacing) to display the study site. The yellow square is the approximate location of EROS and IKONOS stereo images (12 by 12 km). Note (A) the melting snow in the mountains; (B) frozen lakes; (C) lakes with significant melting ice; (D) ski areas with snow. SPOT Image © CNES, 2003; Courtesy of SPOT-IMAGE.


**Figure 2.** Sub-image of backward image of the IKONOS stereo pair, north of Québec City, Quebec, Canada. Note (A) tree shadows and (B) mountain shadows due19° solar elevation angle and 166° azimuth angle and (C) a skater on a frozen lake. IKONOS Image © Space Imaging LLC, 2001.

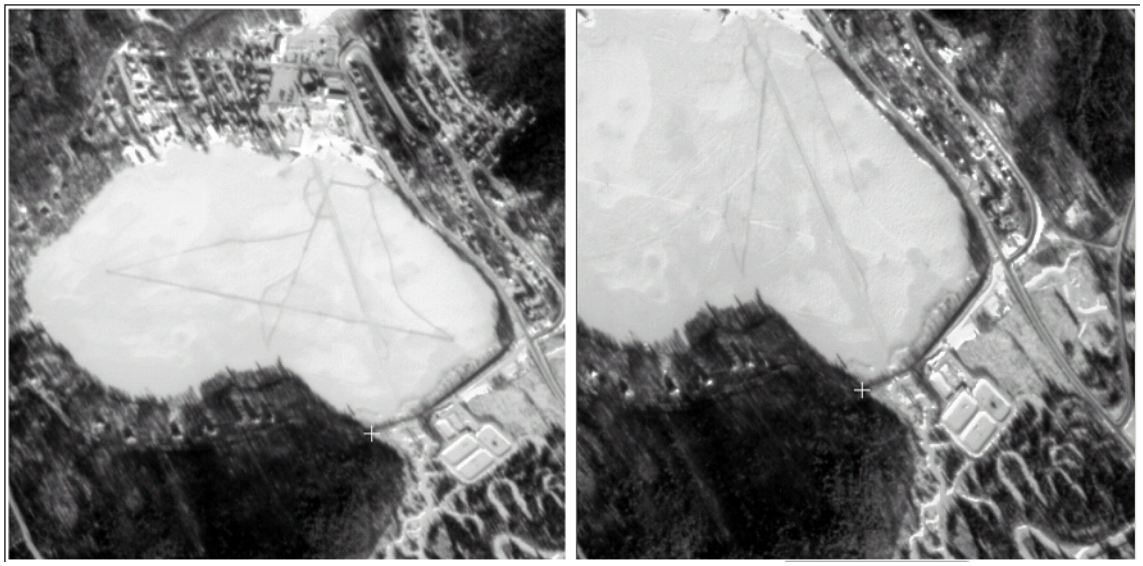

**Figure 3.** Example of the asynchronous EROS-A sub-images (512 x 512 pixels) acquired over Quebec, Canada. Note the shape/size variations of the lake, skidoo tracks and roads. EROS Images © and courtesy ImageSat Intl., 2002.

### 2.2 3-D CCRS Physical Model

The 3-D CCRS physical model was originally developed to suit the geometry of push-broom scanners, such as SPOT-HRV and subsequently adapted as an integrated and unified geometric modeling to geometrically process multi-sensor images. In summary, the geometric modelling represents the well-known collinearity condition (and coplanarity condition for stereo-model), and takes into account the different distortions relative to the global geometry of viewing, i.e. (Toutin, 2003):

- the distortions relative to the platform (position, velocity, orientation);
- the distortions relative to the sensor (orientation angles, instantaneous field of view, detection signal integration time);
- the distortions relative to the Earth (geoid-ellipsoid including elevation); and
- the deformations relative to the cartographic projection (ellipsoid - cartographic plane).

This 3-D physical model has been applied to visible and infrared (VIR) data (Landsat-5 and Landsat-7, SPOT-1-4, IRS, ASTER, KOMPSAT, MERIS), HR VIR data (SPOT-5, EROS-A, IKONOS and QuickBird), as well as radar data (ERS-1/2, JERS, SIR-C, RADARSAT, ENVISAT and airborne SAR) with three to six GCPs. This 3-D physical model applied to different image types is robust and not sensitive to GCP distribution if there is no extrapolation in planimetry and elevation (Toutin, 2003). Based on good quality GCPs, the accuracy of this model is within one-third of a pixel for medium-

resolution VIR images, one pixel or better for HR images and one resolution cell for radar images.

### 2.3 Processing Steps of DEM Generation

Since the processing steps of DEM generation from HR stereo images are roughly the same than for other stereo images (data collection and pre-processing, stereo bundle adjustment with GCPs, elevation parallax measurements, DEM generation and edition), the five processing steps are only summarized:

1. Acquisition and pre-processing of the remote sensing data (images and metadata) to determine an approximate value for each parameter of 3-D physical model for the two images;

2. Collection of stereo GCPs with their 3-D cartographic coordinates and two-dimensional (2-D) image coordinates. GCPs covered the total surface with points at the lowest and highest elevation to avoid extrapolations, both in planimetry and elevation. The image pointing accuracy was around half-pixel for SPOT-5, one pixel for EROS-A and one to two pixels for IKONOS.

3. Computation of the 3-D stereo model, initialized with the approximate parameter values and refined by an iterative least squares bundle adjustment with the GCPs (Step 2) and orbital constraints.

4. Extraction of elevation parallaxes using multi-scale mean normalized cross-correlation method with computation of the maximum of the correlation coefficient;

5. Computation of *XYZ* cartographic coordinates from elevation parallaxes in a regular grid spacing (Step 4) using the previously-computed stereo-model (Step 3) with 3-D least squares stereo-intersection.

After some blunder removal, the DEMs are evaluated with the lidar elevation data. About five to six millions of points corresponding of the overlap area between the stereo-pair and the lidar coverages were used in the statistical computation of elevation errors. Different parameters (land cover and its surface height, terrain relief and slope), which have an impact on elevation errors, were also evaluated.

## 3 RESULTS AND DISCUSSIONS

Error propagation can be tracked along the processing steps with stereo-bundle adjustment results (Step 3), and during the DEM generation (Steps 4 and 5). For these two last steps,

qualitative results are given for each stereo-pair, but the quantitative results on DEMs are only given, where lidar elevation data (5 by 13 km) was acquired.

### 3.1. Stereo-Bundle Adjustment Results

10 GCPs were used for SPOT-5 and IKONOS because previous results demonstrated that it was a good compromise with this dataset to avoid the propagation of input data error (cartographic and image pointing) into 3-D physical stereo-models (Toutin, 2003). More GCPs were used with EROS-A due to its asynchronous orbit. The remaining points as ICPs, which were not used in the 3-D stereo-model calculations, enabled to perform unbiased validations. Table II summarizes these results: the root mean square (RMS) residuals on 10/18 GCPs and the RMS errors ICPs. The RMS *Z* residuals, as *a priori* DEM accuracy, reflect approximately the image pointing errors (2-3 m for SPOT-5; 4 m for EROS and 1-2 m for IKONOS) with *B/H* of one. When compared to the resolution, SPOT achieved the best results (sub-pixel) while EROS achieved the worse (two pixels). The main reasons are the strongest stability of synchronous versus asynchronous satellites but also the 820-km altitude for SPOT (less orbital perturbations) versus the 500-600 km altitude for EROS and IKONOS. Since these RMS errors mainly include the extraction error of ICP features, the internal accuracy of stereo-models is then better, in the order of sub-pixel for SPOT and IKONOS and one pixel for EROS.

Table II: Stereo-bundle adjustment results (in metres) computed with 10/18 GCPs: the root mean square (RMS) residuals and the RMS errors on ICPs.

| Stereo-Bundle | Number of GCPs/ICPs | RMS GCP Residuals | | | RMS ICP Errors | | |
|---|---|---|---|---|---|---|---|
| | | X | Y | Z | X | Y | Z |
| **SPOT-5** | 10/23 | 1.5 | 1.4 | 1.3 | 2.6 | 2.2 | 2.9 |
| **EROS-A** | 18/112 | 2.4 | 2.8 | 3.8 | 4.2 | 4.2 | 5.9 |
| **IKONOS** | 10/45 | 1.2 | 1.6 | 1.9 | 2.4 | 2.1 | 3.0 |

### 3.2 DEM Evaluation Results

The second result is the qualitative evaluation of the full DEMs and the quantitative evaluation of DEMs with the lidar. Fig. 4 is the full DEM (60 x 60 km; 5-m grid spacing) extracted from SPOT-5, which well reproduces the terrain relief and different features (Fig. 1), such as the mountains and valleys, the St Lawrence River and the large island. Even some small relief features were captured between the mountains in the North and the St Lawrence valley. The black areas correspond to mismatched areas due to radiometric differences between the multidate images due to (A) melting snow in the mountains and forests, (B) frozen lakes or with significant melting ice and (C) the St Lawrence River.

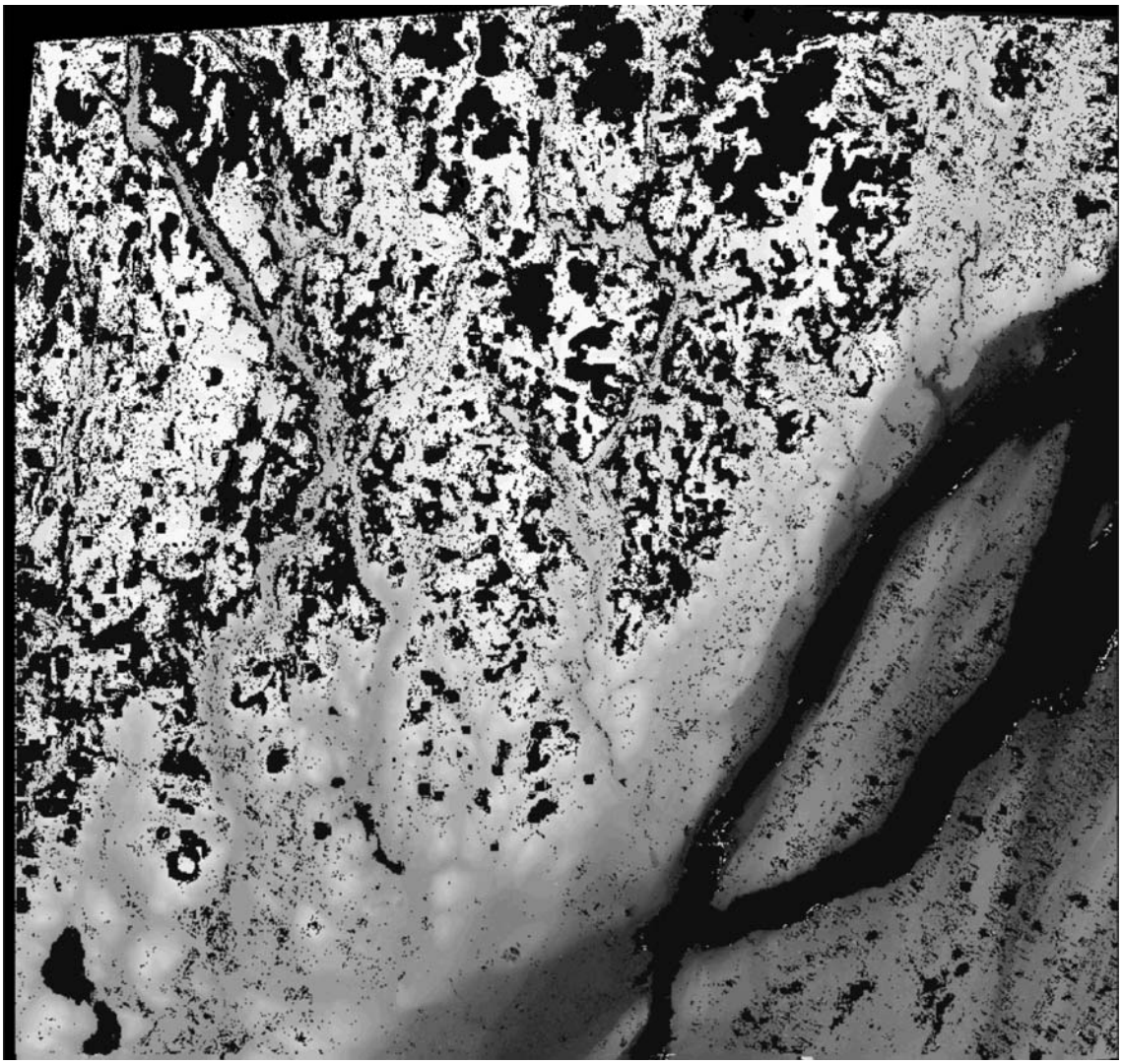

**Figure 4.** DEM (60 x 60 km; 5 m spacing) extracted from the two SPOT-5 stereo pairs. The black areas correspond to matching errors generated from radiometric differences between the multidate images: due to melting snow in the mountains, frozen lakes and the St Lawrence River (see Fig. 1).

Fig. 5 is the full DEM (13 x 13 km; 2-m grid spacing) extracted from EROS-A, which reproduces the general features of the terrain relief, such as the small mountains in the center but not the smallest topographic details. Conversely to multi-date SPOT DEM, the mismatched areas (in black), mainly located in the top of the stereo pair are not due to snow cover and frozen lakes but to a combination of two other factors, which have generated uncertainty and errors in the matching process: (1) the pixel spacing (geometric factor) of both images are quite different (20%) and (2) the area covered by forest do not included well defined features with 2-m resolution (radiometric factor). When one of these factors is absent, the matching process performed well: either in the

centre of the stereo-pair where there is forest but the image pixels are more identical, or in the bottom of the stereo-pair where there are 20% pixel-spacing differences but well-defined features of residential areas.

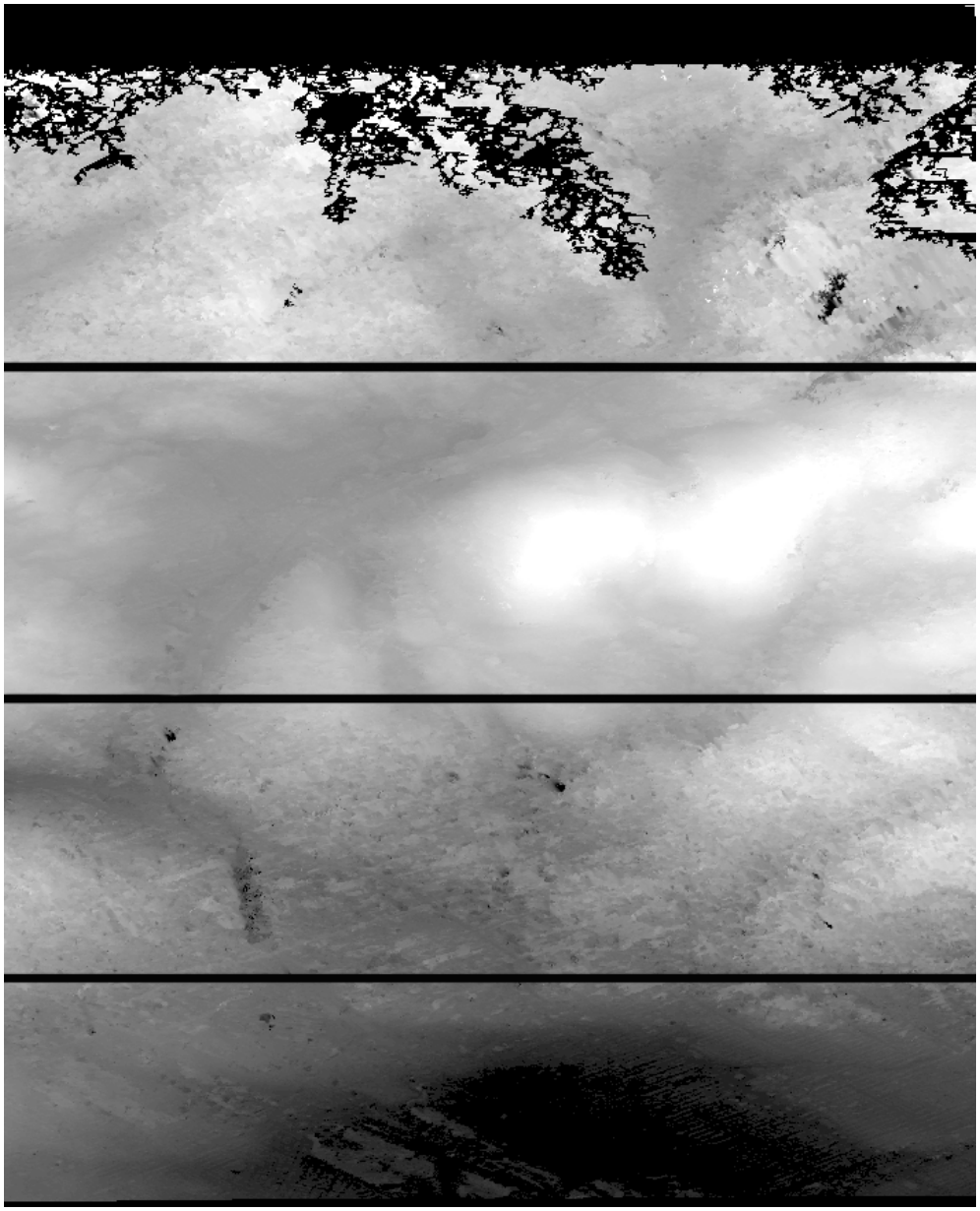

**Figure 5.** DEM (13 x 13 km; 2 m spacing) extracted from the EROS stereo pairs. Large mismatched areas occurred in the top of the stereo pairs due to a combination of two factors: differences of pixel of the stereo-images and forest coverage. The DEM is cut into four horizontal parts according to the matching score results for the evaluation of the elevation accuracy.

Fig. 6 is the full DEM (10 x 10 km; 1-m pixel spacing) extracted from IKONOS, which well reproduces the full terrain relief with high topographic details but also different cartographic features. Specific features visible on the IKONOS images are also identifiable on the DEM due to elevation differences: sand/gravel pits in A; some patterns in B related to streets/houses in residential areas; linear features in C related to main roads and power-line clearcut in the forest environment and lakes in D. Even though the images were acquired in January with snow cover and frozen lakes there are only few mismatched areas, of which includes lakes. The good matching performance over the lakes is due to some texture/contrast and tracks of the snowmobiles and skaters (Fig. 2). The remaining mismatched areas are mainly located in the northwest slopes of mountains (Fig. 2) due to the solar shadow (elevation angle of 19º and azimuth of 166º).

The quantitative evaluation was with the comparison with the lidar elevation data and five to six millions of points were used in the statistical computations. Table III gives the results computed from elevation errors for the three DEMs: the linear errors with 68% and 90% levels of confidence (LE68 and LE90, respectively), the bias and the percentage of class over three times LE68 (in metres).

The general results for SPOT-5, EROS and IKONOS (LE68 of 6.5 m, 20 m and 6.4 m) are respectively, good, poor and medium results when compared to the stereo bundle adjustment RMS *Z*-residuals (Table II), but also in relation with the pixel spacing for each stereo-pair (1.8 m, 5 m and 1 m, respectively) and a *B/H* of one. For EROS the 20-m LE68 errors were mainly due to the same problems previously mentioned for the mismatched areas. In order to confirm this hypothesis, the DEM was cut into four horizontal parts (Fig. 5) according to matching score results. New elevation statistics were computed for each part and LE68 of 45 m, 10 m, 15 m and 10 m from top to bottom were obtained. The best results, however, correspond to "4-pixel" accuracy.

For SPOT-5, 6.5-m LE68 corresponds to an image matching error of ±1.3 pixel (*B/H* of one), which is close of previous results generally achieved with different VIR and radar stereo-images ("one-pixel" image matching accuracy) (Gülch, 1991). The 6.4-m LE68 results with IKONOS (1-m pixel spacing) theoretically correspond to a worse image matching performance (about 6 pixels). The largest errors (three times LE68) for both DEMs, although they only represent very small percentage, are out of tolerance and cannot be acceptable in a topographic sense. These largest errors, however, are generally located in the different shadow areas due to mountains, trees or buildings, and some (15-20 m) result from the elevation comparison of canopy versus ground elevations due to the different spatial resolutions of SPOT/IKONOS and lidar data and due to the different acquisition seasons (leaves or no leaves). Consequently. these errors are representative of our stereo-images (acquired in winter) and experiment (lidar data acquired in summer), but not of the general SPOT/IKONOS stereo-performance for DEM generation.

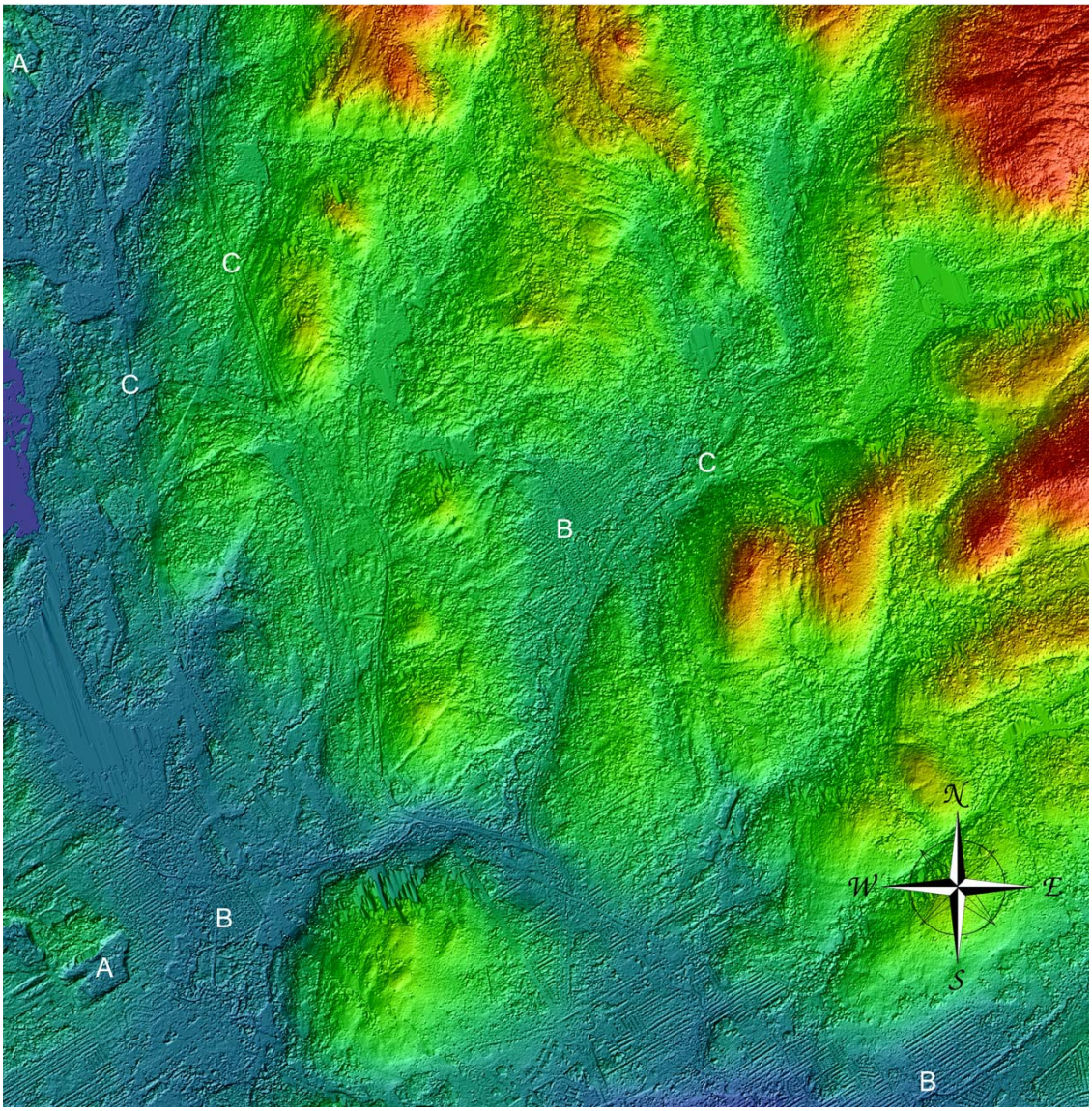


**Figure 6.** DEM (10 x 10 km; 1 m spacing) extracted from the IKONOS stereo pair. Due to surface elevations cartographic features are well noticeable: (A) sand pits, (B) residential areas, (C) roads and power lines, (D) lakes. The linear features, which occur in residential areas (B), are not artefacts or systematic errors but are related to streets and houses patterns.

In fact, SPOT/IKONOS DEMs are digital surface models (DSMs), which include the elevation of natural and human-made surfaces (trees, houses, hedges, etc.). The more accurate is the DEM the more noticeable are the elevation of some surfaces and the more distinguishable are the resulting cartographic features (sand pits, transportation networks, residential areas, see Fig. 6). It explains why surface elevations were not noticeable on the medium-accurate EROS DEM. Consequently, these two DSMs are evaluated on bare soils and lakes. The results (2.2 m and 1.5 m LE68) for SPOT and

IKONOS respectively, are now more consistent with *a priori* 3-D restitution accuracy from the stereo bundle adjustment (2 m in *Z*) and better reflect their potential for DEM generation. While "half-pixel" accuracy is achieved for SPOT, it is only "1.5 pixel" accuracy for IKONOS. The potential reasons should be the use of raw SPOT data (original geometry and radiometry) while IKONOS were processed as a map-oriented product resulting in a "non-original" geometry and a resampled radiometry. Finally SPOT/IKONOS DEMs were evaluated over different forest classes (deciduous, conifer, mixed, sparse). The results (4 m to 6.6 m LE68) for the different forests are coherent with the nature of each forest class taking into account the season variation between SPOT and IKONOS images and lidar acquisitions and an estimation of tree heights (15-20 m and 10-15 m for the deciduous and conifers, respectively) in this study site. These class results explained the general results (around 6.5 m LE68) over full DEMs because the forested areas represent 85% of the total area.

Table III: Statistical results from the comparison of each stereo DEM (SPOT-5, EROS and IKONOS) and the lidar elevation data: linear errors with 68% and 90% levels of confidence (LE68 and LE90, respectively), bias and percentage of the class over three times LE68.

| Stereo-Images | LE68 | LE90 | Bias | Over three LE68 |
|---|---|---|---|---|
| **SPOT-5** | 6.5 m | 10 m | 2 m | 0.7% |
| **EROS-A** | 20 m | 31 m | 3 m | 3.7% |
| **IKONOS** | 6.4 m | 10 m | 6 m | 0.1% |

## 4. Acknowledgements

The author thanks R. Matte (*Ministère des Ressources naturelles du Québec*, Canada) for the topographic data; GPR Consultants (Québec, Canada) for the lidar survey; R. Chénier (Consultants TGIS inc., Canada), S. Grassi (Università degli Studi Perigia, Italy) for data processing.

## 5. References

Bouillon, A., Breton, E., Lussy, F. de, and Gachet R. (2002) SPOT5 HRG and HRS first in-flight geometric quality results, in *Proc. of SPIE, Vol. 4881A Sensors, system, and Next Generation Satellites VII,* Agia Pelagia, Crete, Greece, 22-27 September 2002, CD-ROM (Paper 4881A-31).

Chen, L.-C. and Teo, T.-A. (2002) Rigorous Generation of Orthophotos from EROS-A High Resolution Satellite Images, *International Archives of Photogrametry and Remote Sensing and Spatial Information Sciences*, Ottawa, Canada, July 8-12, vol. 34 ( B4), pp. 620-625.

Dial, G. (2000) IKONOS Satellite Mapping Accuracy, in *Proc. ASPRS Congress*, Washington DC, USA, 26 May 2000, CD-ROM.

Gülch, E. (1991) Results of Test on Image Matching of ISPRS WG III/4, *ISPRS J. Photogramm. Remote Sens.*, vol. 46, no. 1, pp. 1-8.

Toutin, Th. (2000) Elevation modeling from satellite data, *Encyclopedia of Analytical Chemistry: Applications, Theory and Instrumentation* (R. A. Meyers, editor), vol. 10, John Wiley & Sons, Ltd., Chichester, UK, pp. 8543-8572, URL: http://www.ccrs.nrcan.gc.ca/ccrs/rd/sci_pub/bibpdf/4622.pdf.

Toutin, Th. (2003) Error tracking in IKONOS geometric processing using a 3D parametric modelling, *Photogramm. Eng. Remote Sens.*, vol. 69, no. 1, pp.43-51. URL: http://www.ccrs.nrcan.gc.ca/ccrs/rd/sci_pub/bibpdf/13102.pdf.